photonics

MDPI

Article

Generation of Tunable Plasmonic Vortices by Varying Wavelength of Incident Light

Yihua Bai, Qing Zhang * and Yuanjie Yang *

School of physics, University of Electronic Science and Technology of China, Chengdu 611731, China
* Correspondence: qingzhang@uestc.edu.cn (Q.Z.); dr.yang2003@uestc.edu.cn (Y.Y.)

Abstract: Surfaces plasmon polaritons carrying orbital angular momentum (OAM), known as plasmonic vortex, hold potential applications for on-chip information multiplexing. However, a traditional plasmonic vortex lens was usually designed for monochromatic incident light and encountered challenges in generating multiple vortices. Here, we demonstrated a wavelength-tunable plasmonic vortex generator that ameliorates these limits, relying on the simultaneous design of a geometric metasurface on an Archimedean spiral. Through this design strategy, both the topological charges and the location of vortices can be controlled with different wavelengths of incident beams. This design and concept can preserve incident wavelength information and can be further applied to integrated and high-dimensional on-chip devices.

Keywords: orbital angular momentum; plasmonic vortex; surface plasmon polaritons; plasmonic metasurface

Citation: Bai, Y.; Zhang, Q.; Yang, Y. Generation of Tunable Plasmonic Vortices by Varying Wavelength of Incident Light. *Photonics* **2022**, *9*, 809. https://doi.org/10.3390/photonics9110809

Received: 12 October 2022
Accepted: 25 October 2022
Published: 27 October 2022

1. Introduction

Light beams can possess both spin angular momentum (SAM) and the orbital angular momentum (OAM) that are manifested as circular polarization and helical phase distribution, respectively [1]. A vortex beam with an azimuthal phase term $\exp(il\theta)$ carries the OAM of $l\hbar$ per photon, where θ is the azimuthal angle and l is the topological charge [2]. The unique characteristics of vortex beams have initiated appreciable interest [3–6], ranging from optical tweezers [7,8] and quantum entanglement [9,10] to optical communications [11,12]. Nevertheless, practical applications of conventional optical vortex beams, the ability to manipulate objects at nanoscale for instance, are restricted due to the diffraction limit of light. More recently, surface plasmon polaritons (SPPs) vortices have been widely studied owing to their prominent properties [13,14], holding great potential to overcome those obstacles and control small particles with higher precision [15].

SPPs are propagated evanescent waves that arise from the coupling of collective oscillations of electrons with the photon of incident lights. Analogous to free-space optical vortex, SPPs are capable of carrying OAM and exhibit a great ability to create the field enhancement, known as plasmonic vortices [16,17]. The topological charge of plasmonic vortices is dependent on its phase singularity and phase structure, namely, the same as that of optical vortex beams. Generally, plasmonic vortices are generated by spiral nanostructures on metal, where the azimuthal phase originates from the optical path variation with the winding configurations. For instance, the Archimedean spiral is likely one of the most simple structures with which to generate plasmonic vortices [18–20]. For a fixed Archimedean-spiral structure, monochromatic incident light is usually used to excite SPPs, leading to the generation of a specific plasmonic vortex at the center. However, such traditional plasmonic vortex generators are static, making them unsuitable for OAM modulation and multiplexing limited by their strong dependence on the structure and composition of the surface.

Recently, the manipulation of vortex beams has been studied as a vital research topic for applications in both quantum and classical realms. To further increase the degree of

freedom, the concept of the Pancharatnam–Berry (PB) phase in the metasurface is adopted in the designing of a vortex generator [21,22]. By modulating the orientation of anisotropic meta-atoms such as rectangular slits, the topological charge and location of the launched SPP vortex can be precisely controlled [23]. Note that the SAM of the illumination interacts with the structure, thus the coupling SPPs are polarization-responsive [24,25]. Moreover, superposition of two SPP OAM states and complex structured patterns were realized by the use of plasmonic metasurfaces [26]. Additionally, multiple optical vortices were excited in a phyllotaxis-inspired nanosieve [27]. However, in those cases, SPP waves with different OAM modes were concentrically generated at the same position, while the excitation of plasmonic vortices at diverse locations has been scarcely reported, especially for a single plasmonic lens. Superposition of structures or more complicated designs could be required to achieve multiple vortices generation [28,29]. Lately, photonic spin Hall lens controlled by the handedness of incident light was proposed, which consisted of two plasmonic lenses that respond to left- and right-handed circular polarized lights, respectively [30]. Two plasmonic vortices can be produced by illuminating lights with two different circular polarizations. Notwithstanding, a few plasmonic metasurfaces have been proposed to produce SPP vortices based on the PB phase elements; in such a configuration, the distance between the paired rectangular nanogrooves is generally set as half the wavelength of the SPP wave. To date, the influence of the distance on generated plasmonic waves has not been reported. More importantly, a fixed metasurface is usually limited to an appointed incident wavelength. This highly impairs the usefulness of plasmonic metasurfaces. Therefore, it is urgent to demonstrate a wavelength-dependent plasmonic lens that aims for SPP vortices generation.

In this paper, we present a tunable plasmonic vortex generator that couples polychromatic illumination into SPP vortices with different topological charges while allowing full control over the corresponding distance shift. The wavefronts of launched SPPs can be manipulated simultaneously by the dynamic phase from the global structure of the Archimedean spiral, as well by the local PB phase from each meta-slit. Such a dual-phase arrangement thus enables multiple plasmonic vortex generation in a single device. The location and topological charge of the stimulated plasmonic wave are strongly dependent on the distance between the paired atoms of the metasurface. Only centrally-located plasmonic vortex can be generated with spacing being integer multiple of the SPP wavelength, whereas its location can be also controlled through PB phase with spacing of half the SPP wavelength. More significantly, the generated vortices can be controlled by varying the wavelength of the incidence. Our results provide an extra degree of freedom to manipulate SPP waves and exhibit the potential for on-chip photonic technologies.

2. Methods

The schematic of our wavelength-controlled tunable plasmonic vortex generator is shown in Figure 1a. For a specific structure, an SPP vortex can be excited at the center under illumination of a circularly polarized light with λ = 532 nm, while another vortex with a different topological charge can be generated with a spatial shift when the wavelength of incidence changes to 1064 nm. Particularly, we can obtain dual vortices by tuning the wavelength to 633 nm. As shown in Figure 1b, the device can be achieved by an Archimedean spiral structure arranged with orthogonally distributed rectangular slits; the SPPs launched from each slit can be regarded as a dipole that propagates perpendicularly to the center.

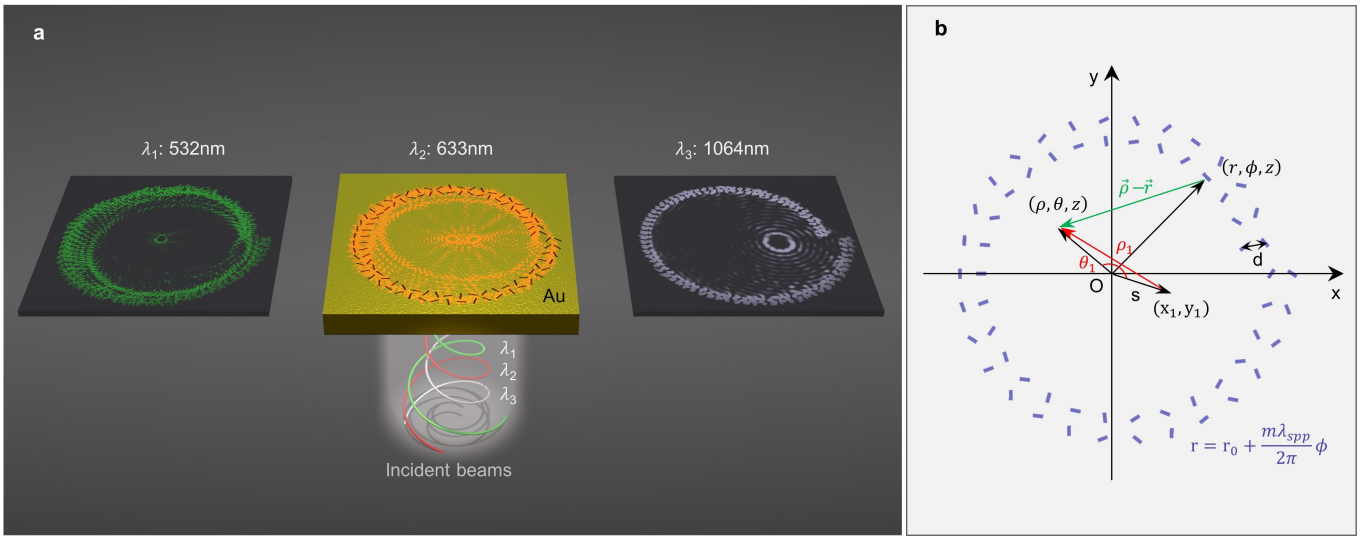

Figure 1. Tunable excitation of SPP waves carrying OAM. (**a**) Schematics of a plasmonic vortex generator. The launched SPP waves with varying topological charges at a predesigned location can be generated by illuminating light with different wavelengths (green: 532 nm, red: 633 nm, grey: 1064 nm). (**b**) Schematic diagram of the plasmonic metasurface, with the phase controlled by the orientation of paired perpendicular nanoslits.

It is generally accepted that SPPs carrying OAM can be excited when a metal film etched with an Archimedean spiral, $r = r_0 + m\lambda_{spp}\phi/2\pi$, is illuminated with a circularly polarized beam [31]. Here, r_0 is the initial distance, ϕ is the azimuthal coordinate and m is the geometrical topological charge, denoting the ratio of spiral pitch to the SPP wavelength λ_{spp}. Periodic phase change can be introduced into the SPPs originating from different locations of the spiral, giving rise to a plasmonic vortex. Under illumination of a circularly polarized beam, the electric field at the observation point (ρ, θ, z) can be written as [30,32]:

$$\begin{aligned} E_{spp}(\rho,\theta,z) = A_0 \exp(-\kappa_z z) \int \Big\{ & \cos[(n-1)\phi] \\ & - \sin[(n-1)\phi] \exp(\frac{i\sigma\pi}{2}) \exp(ik_{spp}d) \Big\} \\ & \times \exp(in\sigma\phi) \exp(ik_{spp}[r - \rho\cos(\theta-\phi)])\mathrm{d}\phi, \end{aligned} \tag{1}$$

where κ_z is the attenuation coefficient, $k_{spp} = 2\pi/\lambda_{spp}$ is the wavenumber of SPPs and n is the rotation factor that denotes the rotation angle of slits changes $2n\pi$ during one revolution. We consider a pair of orthogonally distributed rectangular slits that are spaced a distance $d = N\lambda_{spp}/2$ apart as a meta-atom, the corresponding electric field can be expressed as:

$$\begin{aligned} E_{spp}(\rho,\theta,z) =& A_0 \exp(-\kappa_z z) \int \exp\Big\{ i\Big(\sigma[(-1)^{N+1}(n-1)+n]+m\Big)\phi \Big\} \\ & \times \exp\Big\{ ik_{spp}[r_o - \rho\cos(\theta-\phi)] \Big\} \mathrm{d}\phi \\ & \propto \exp(-\kappa_z z) \exp\Big\{ i\Big(\sigma[(-1)^{N+1}(n-1)+n]+m\Big)\theta \Big\} \\ & \times J_{\sigma[(-1)^{N+1}(n-1)+n]+m}(k_{spp}\rho), \end{aligned} \tag{2}$$

where the integral form of the Bessel function has been used and $J_t(\alpha)$ is a t-order Bessel function of the first kind. With this geometry, SPP waves carrying OAM can be generated at the center of structure, the topological charge of which is related to the SAM of incidence

σ, the structure of spiral m, the rotation factor n, as well as the spacing of the meta-atom d. To generate an SPP vortex at position (x_1, y_1), Equation (2) can be further deduced as:

$$\begin{aligned} E_{spp} &\propto \exp(-\kappa_z z)\exp\left\{i\Big(\sigma[(-1)^{N+1}(n-1)+n]+m\Big)\theta\right\} \\ &\quad \times J_{\sigma[(-1)^{N+1}(n-1)+n]+m}(k_{spp}\rho_1) \\ &\propto \begin{cases} \exp(-\kappa_z z)\exp[\sigma(2n+1)+m]J_{\sigma(2n+1)+m}(k_{spp}\rho_1) & \text{if } N \text{ is odd} \\ \exp(-\kappa_z z)\exp(\sigma+m)J_{\sigma+m}(k_{spp}\rho_1) & \text{if } N \text{ is even,} \end{cases} \end{aligned} \tag{3}$$

where $\rho_1 = \sqrt{(x-x_1)^2+(y-y_1)^2}$. Notably, the topological charge of the plasmonic vortex is $\sigma + m$ with N being an even number, which is merely dependent on the polarization state of illuminating beam σ and the spiral pitch of the structure $m\lambda_{spp}$. In this case, owing to its topological charge being irrelevant to the rotation factor n, the launched SPP wave cannot be controlled by the PB phase of the metasurface, thus only a centrally-located plasmonic vortex can be generated.

Based on the spacing of the orthogonal rectangular slits d, the intensity distribution of SPP waves with optional location shift as predicted by Equation (3) was studied. Simulations were performed with the finite-difference time-domain method, the wavelength of incident light was λ = 660 nm, corresponding to $\lambda_{spp} \cong 634$ nm. The width and length of rectangular slits were set as 100 nm and 400 nm, respectively. The thickness of the gold film was 100 nm, the geometrical topological charge was $m = 1$, and the rotation factor was $n = 1$. Moreover, this structure mainly excited the E_z component of SPPs and other components could be neglected. Figure 2a shows that a structure with $d = \lambda_{spp}$ results in an SPP vortex at the origin of coordinates, the topological charge of which is $l_1 = \sigma + m = 2$. Remarkably, a plasmonic vortex with $l_2 = \sigma(2n-1) + m = 2$ can be obtained at a predesigned position by modulating the PB phase only when the spacing is half the SPP wavelength ($d = \lambda_{spp}/2$), as shown in Figure 2c.

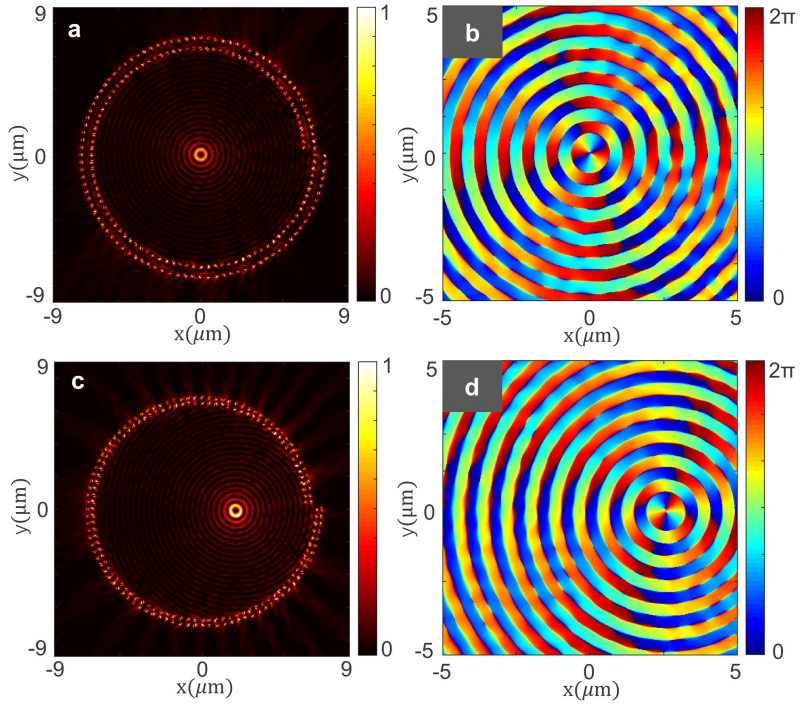

Figure 2. Generation of the tunable plasmonic vortices through varying spacing of the paired nanoslits. (**a**) Intensity and (**b**) phase distribution of the SPP wave with the distance $d = \lambda_{spp}$, demonstrating the generation of a centrally-located vortex. (**c**,**d**) Same as (**a**,**b**) but the distance $d = \lambda_{spp}/2$.

Switchable location shift is possible by altering the distance between the meta-atom, and the required phase profile of the elongated nanoslits can be illustrated as:

$$\begin{aligned}\varphi(\theta) =& \frac{2\pi}{\lambda_{spp}}\left[\rho + s - \sqrt{\rho^2 + s^2 - 2\rho s\cos(\theta - \theta_1)}\right] \\ &+ \left\{\sigma[(-1)^{N+1}(n-1) + n] + m\right\}\theta,\end{aligned} \tag{4}$$

where $\theta_1 = \arctan[(y - y_1)/(x - x_1)]$, $\rho = \sqrt{x^2 + y^2}$, and $s = \sqrt{x_1^2 + y_1^2}$ denotes the location shift of the eccentric vortex. When the spacing d is an integer multiple of λ_{spp}, the launched SPP waves become independent of the PB phase of the plasmonic metasurface, viz., the rotation factor of the structure n.

3. Results and Discussion

Aside from the two specific circumstances above, the spacing d can be any value between them. To further study the influence of the spacing between the paired perpendicular slits on generated plasmonic vortices, we subsequently performed similar simulations with different spacings. The eccentric SPP vortex gradually evolves into two vortices with the d changing from 0.5λ to 0.75λ, and degenerates into one again when d keeps increasing to λ_{spp}. In Figure 3, the intensity distribution of the dual vortices is compared. In the case of $d = 0.75\lambda_{spp}$, as an equal superposition of two situations in Figure 2, equivalent excitation of both vortices is observed. For $d = 0.65\lambda_{spp}$ ($d = 0.85\lambda_{spp}$), however, the off-center vortex (central vortex) is predominantly excited. Note that the primary ring sizes of vortices ($l = 2$) and the location shift are the same in all cases, which is coincident with Figure 2. Moreover, it clearly indicates that the location of the stimulated plasmonic wave can be controlled through the PB phase rather than the spiral structure itself. The Archimedean spiral can only excite one vortex at the center, and the other vortex can be generated at different locations in the inner spiral as predesigned by the PB phase.

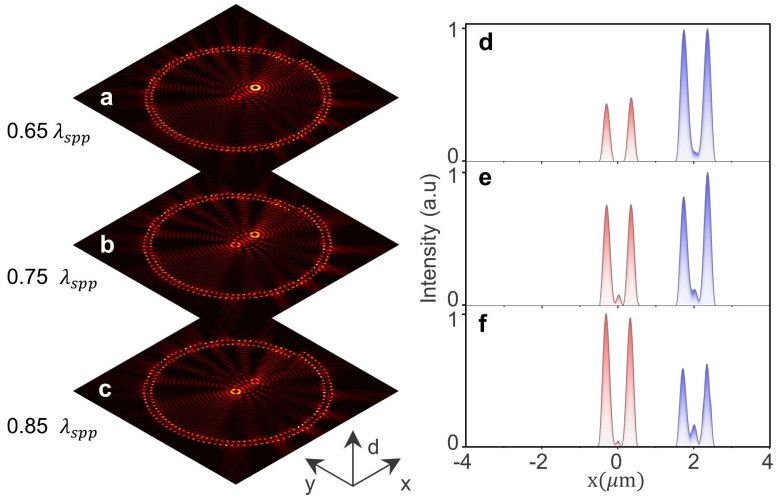

Figure 3. Excitation of dual vortices with an Archimedean-spiral-shaped plasmonic vortex generator. (**a**–**c**) Intensity distributions of launched SPP waves for different d under illumination of a right-handed circularly polarized light. (**d**–**f**) Normalized cross-sections of the intensity profiles at y = 0, showing the dependence of excited SPP vortices on the spacing of each paired slit.

This scheme can be generalized to a wavelength-controlled SPP coupler, where a fixed spacing d in the structure for one specific wavelength weighs diversely for other incidences. Depending on the ratio of d to the corresponding λ_{spp}, different wavelengths result in SPP waves carrying various topological charges at varying locations. Given a structure designed for an illuminating beam (λ = 1064 nm), the geometric topological charge of the

spiral is $m = 4$. The perpendicular slits were spaced $d = \lambda_{spp}(1064\text{ nm})$ apart, and other parameters were the same as above. Here, we performed simulations of SPPs emanated by the specified generator for various incident wavelengths. The device was back-illuminated with right-handed circularly polarized beams, and the interference of SPPs was observed at a distance of 100 nm over the interface.

In Figure 4a, we illustrate the intensity distribution of SPP waves excited by the illumination with a free space wavelength of 1064 nm, where a central vortex is observed as expected. In the case of an incident wavelength of 2100 nm, the spacing d is nearly half the wavelength of SPPs $\sim\lambda_{spp}(2100\text{ nm})/2$, thus a deviating vortex is exhibited in Figure 4c. For incidence with a wavelength of 1523 nm, similar to the case of d = $0.75\lambda_{spp}$, dual vortices are shown in Figure 4b. Moreover, Figure 4d–f present corresponding phase profiles for these three cases, in which the white dashed circles indicate the existence of SPP vortices. In order to manifest accurate wavelength responses of such a vortex generator, the topological charge and the location shift were analyzed in detail. Figure 4g shows that, for λ_{in} = 1064 nm, the topological charge of the central vortex equals $l_1 = \sigma + m = 5$, whereas an incidence of λ_{in} = 2100 nm launches SPP beams with $l_2 = \sigma(2n-1) + m' = 3$ due to the spiral pitch of the structure $m\lambda_{spp}(1064\text{ nm}) = m'\lambda_{spp}(2100\text{ nm})$, denoting that the geometric topological charge is $m' = 2$. For the incidence with λ = 1523 nm, owing to the fact that $m'' \approx 3$ in the structure $m\lambda_{spp}(1064\text{ nm}) = m''\lambda_{spp}(1523\text{ nm})$, we can observe one vortex with $l_1 = \sigma + m'' = 4$ and the other vortex with $l_2 = \sigma(2n-1) + m'' = 4$.

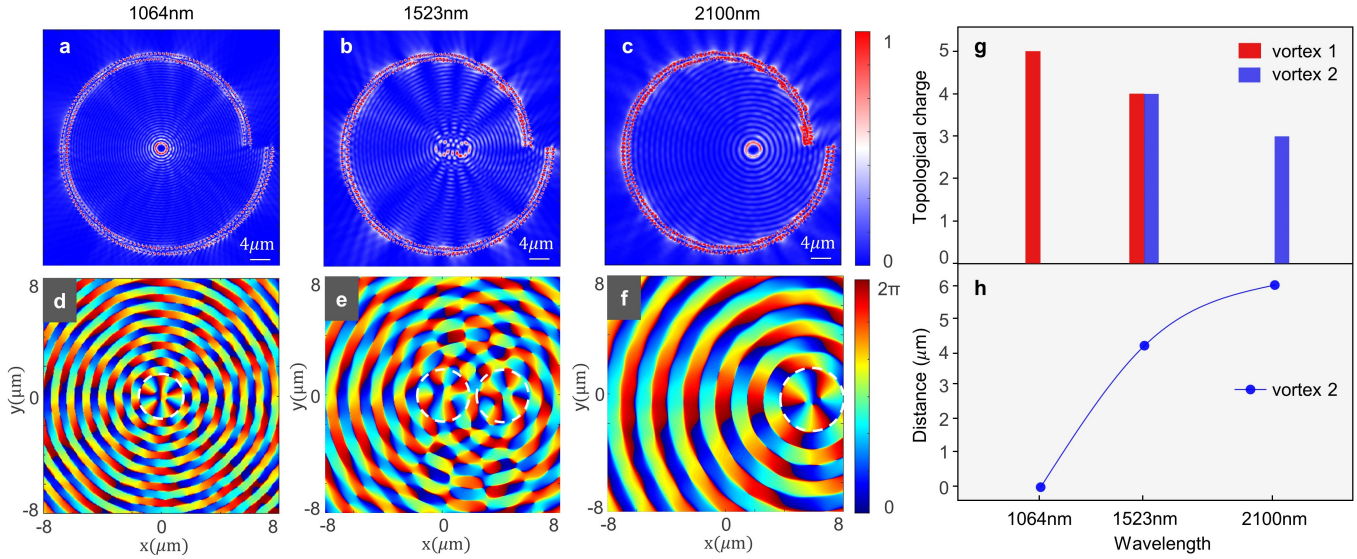

Figure 4. Tunable excitation of plasmonic vortices upon illumination with different wavelengths, where (**a**,**d**) 1064 nm, (**b**,**e**) 1523 nm and (**c**,**f**) 2100 nm, respectively. Intensity (**a**–**c**) and phase (**d**–**f**) profiles of the launched SPPs. The corresponding topological charges (**g**) and location shifts (**h**) of the emanated plasmonic vortices.

Besides an SPP vortex excited at the origin, there is a vortex with a tunable location depending on the wavelength of illumination, the deviation distances of which are plotted by the blue solid line in Figure 4h. In the case of λ_{in} = 1064 nm, the structure was initially designed to generate an SPP vortex at position (12 μm, 0 μm) by controlling the orientation angle of each slit. However, it shows in particular that a structure with spacing $d = \lambda_{spp}$ can only generate a plasmonic vortex at the origin. According to Equation (4), the location shift is inversely proportional to the SPP wavelength λ_{spp}, thus illumination with λ_{in} = 2100 nm launches an SPP vortex at (6 μm, 0 μm). Similarly, a plasmonic vortex is distributed around (4.2 μm, 0 μm) under illuminating beam λ_{in} = 1523 nm. Depending on the wavelength, a vortex generator can be used to achieve tunable excitation of SPP waves carrying different OAMs at an appointed location.

4. Conclusions

In summary, we have demonstrated a general strategy by which dual vortices can be generated based on Archimedean-spiral arranged nano-slit arrays. By exploring the spacing between the paired nano-slits, we thus propose a new degree of freedom—the wavelength of the illuminating beam—as a tool to control the intensity, topological charge and location of a launched polaritonic vortex. We believe that, beyond dual-vortices, the incident wavelength can also be used to achieve other tunable plasmonic devices, such as plasmonic steering and focusing. In addition, our work is capable of preserving the wavelength information of incident beams and also provides potential applications in optical trapping and micromanipulation.

Author Contributions: Conceptualization, Y.B.; methodology, Y.B.; writing—original draft preparation, Y.B., Q.Z. and Y.Y.; writing—review and editing, Q.Z. and Y.Y.; supervision, Q.Z. and Y.Y. All authors have read and agreed to the published version of the manuscript.

Funding: This research was funded in part by the National Natural Science Foundation of China (Nos. 11874102 and 12174047), Sichuan Province Science and Technology Support Program (No. 2020JDRC0006). And supported in part by Sichuan Science and Technology Program (2022YFH0082, and 2022YFSY0023). Q.Z. acknowledges the support from the start-up funding of University of Electronic Science and Technology of China.

Institutional Review Board Statement: Not applicable.

Data Availability Statement: Not applicable.

Conflicts of Interest: The authors declare no conflict of interest.

Abbreviations

The following abbreviations are used in this manuscript:

OAM	orbital angular momentum
SAM	spin angular momentum
SPPs	surface plasmon polaritons
PB	Pancharatnam-Berry

References

1. Yao, A.M.; Padgett, M.J. Orbital angular momentum: Origins, behavior and applications. *Adv. Opt. Photonics* **2011**, *3*, 161–204. [CrossRef]
2. Allen, L.; Beijersbergen, M.W.; Spreeuw, R.J.; Woerdman, J.P. Orbital angular momentum of light and the transformation of Laguerre-Gaussian laser modes. *Phys. Rev. A* **1992**, *45*, 8185–8189. [CrossRef]
3. Jian, C.; Chenhao, W.; Qiwen, Z. Engineering photonic angular momentum with structured light: A review. *Adv. Photonics* **2021**, *3*, 064001.
4. Andrew, F. New twist to twisted light. *Adv. Photonics* **2022**, *4*, 030501.
5. Bai, Y.; Lv, H.; Fu, X.; Yang, Y. Vortex beam: Generation and detection of orbital angular momentum [Invited]. *Chin. Opt. Lett.* **2022**, *20*, 012601. [CrossRef]
6. Buono, W.T.; Forbes, A. Nonlinear optics with structured light. *Opto-Electron. Adv.* **2022**, *5*, 210174–1–210174–19. [CrossRef]
7. Padgett, M.; Bowman, R. Tweezers with a twist. *Nat. Photonics* **2011**, *5*, 343–348. [CrossRef]
8. Yang, Y.; Ren, Y.; Chen, M.; Yoshihiko, A.; Carmelo, R.G. Optical trapping with structured light: A review. *Adv. Photonics* **2021**, *3*, 034001. [CrossRef]
9. Mair, A.; Vaziri, A.; Weihs, G.; Zeilinger, A. Entanglement of the orbital angular momentum states of photons. *Nature* **2001**, *412*, 313–316. [CrossRef]
10. Stav, T.; Faerman, A.; Maguid, E.; Oren, D.; Kleiner, V.; Hasman, E.; Segev, M. Quantum entanglement of the spin and orbital angular momentum of photons using metamaterials. *Science* **2018**, *361*, 1101–1104. [CrossRef]
11. Wang, J.; Yang, J.Y.; Fazal, I.M.; Ahmed, N.; Yan, Y.; Huang, H.; Ren, Y.; Yue, Y.; Dolinar, S.; Tur, M.; et al. Terabit free-space data transmission employing orbital angular momentum multiplexing. *Nat. Photonics* **2012**, *6*, 488–496. [CrossRef]
12. Bozinovic, N.; Yue, Y.; Ren, Y.; Tur, M.; Kristensen, P.; Huang, H.; Willner Alan, E.; Ramachandran, S. Terabit-Scale Orbital Angular Momentum Mode Division Multiplexing in Fibers. *Science* **2013**, *340*, 1545–1548. [CrossRef]
13. Shen, Z.; Hu, Z.J.; Yuan, G.H.; Min, C.J.; Fang, H.; Yuan, X.C. Visualizing orbital angular momentum of plasmonic vortices. *Opt. Lett.* **2012**, *37*, 4627–4629. [CrossRef]
14. Al-Awfi, S. Formation of a Plasmonic Surface Optical Vortex by Evanescent Bessel Light. *Plasmonics* **2012**, *8*, 529–536. [CrossRef]

15. Zhang, Y.; Min, C.; Dou, X.; Wang, X.; Urbach, H.P.; Somekh, M.G.; Yuan, X. Plasmonic tweezers: for nanoscale optical trapping and beyond. *Light. Sci. Appl.* **2021**, *10*, 59. [CrossRef]
16. Ni, J.; Huang, C.; Zhou, L.M.; Gu, M.; Song, Q.; Kivshar, Y.; Qiu, C.W. Multidimensional phase singularities in nanophotonics. *Science* **2021**, *374*, eabj0039. [CrossRef]
17. Bai, Y.; Yan, J.; Lv, H.; Yang, Y. Plasmonic vortices: A review. *J. Opt.* **2022**, *24*, 084004. [CrossRef]
18. Kim, H.; Park, J.; Cho, S.W.; Lee, S.Y.; Kang, M.; Lee, B. Synthesis and dynamic switching of surface plasmon vortices with plasmonic vortex lens. *Nano Lett.* **2010**, *10*, 529–536. [CrossRef]
19. Yang, Y.; Wu, L.; Liu, Y.; Xie, D.; Jin, Z.; Li, J.; Hu, G.; Qiu, C.W. Deuterogenic Plasmonic Vortices. *Nano Lett.* **2020**, *20*, 6774–6779. [CrossRef]
20. Spektor, G.; Prinz, E.; Hartelt, M.; Mahro, A.K.; Aeschlimann, M.; Orenstein, M. Orbital angular momentum multiplication in plasmonic vortex cavities. *Sci. Adv.* **2021**, *7*, eabg5571. [CrossRef]
21. Chen, C.F.; Ku, C.T.; Tai, Y.H.; Wei, P.K.; Lin, H.N.; Huang, C.B. Creating Optical Near-Field Orbital Angular Momentum in a Gold Metasurface. *Nano Lett.* **2015**, *15*, 2746–2750. [CrossRef]
22. Prinz, E.; Spektor, G.; Hartelt, M.; Mahro, A.K.; Aeschlimann, M.; Orenstein, M. Functional Meta Lenses for Compound Plasmonic Vortex Field Generation and Control. *Nano Lett.* **2021**, *21*, 3941–3946. [CrossRef]
23. Zang, X.; Li, Z.; Zhu, Y.; Xu, J.; Xie, J.; Chen, L.; Balakin, A.V.; Shkurinov, A.P.; Zhu, Y.; Zhuang, S. Geometric metasurface for multiplexing terahertz plasmonic vortices. *Appl. Phys. Lett.* **2020**, *117*, 171106. [CrossRef]
24. Lin, J.; Mueller, J.P.B.; Wang, Q.; Yuan, G.; Antoniou, N.; Yuan, X.C.; Capasso, F. Polarization-Controlled Tunable Directional Coupling of Surface Plasmon Polaritons. *Science* **2013**, *340*, 331–334. [CrossRef] [PubMed]
25. Cho, S.W.; Park, J.; Lee, S.Y.; Kim, H.; Lee, B. Coupling of spin and angular momentum of light in plasmonic vortex. *Opt. Express* **2012**, *20*, 10083–10094. [CrossRef] [PubMed]
26. Zhang, Y.; Zeng, X.; Ma, L.; Zhang, R.; Zhan, Z.; Chen, C.; Ren, X.; He, C.; Liu, C.; Cheng, C. Manipulation for Superposition of Orbital Angular Momentum States in Surface Plasmon Polaritons. *Adv. Opt. Mater.* **2019**, *7*, 1900372. [CrossRef]
27. Jin, Z.; Janoschka, D.; Deng, J.; Ge, L.; Dreher, P.; Frank, B.; Hu, G.; Ni, J.; Yang, Y.; Li, J.; et al. Phyllotaxis-inspired nanosieves with multiplexed orbital angular momentum. *eLight* **2021**, *1*, 5. [CrossRef]
28. Zhou, H.; Dong, J.; Zhou, Y.; Zhang, J.; Liu, M.; Zhang, X. Designing Appointed and Multiple Focuses With Plasmonic Vortex Lenses. *IEEE Photonics J.* **2015**, *7*, 1–7. [CrossRef]
29. Moon, S.W.; Jeong, H.D.; Lee, S.; Lee, B.; Ryu, Y.S.; Lee, S.Y. Compensation of spin-orbit interaction using the geometric phase of distributed nanoslits for polarization-independent plasmonic vortex generation. *Opt. Express* **2019**, *27*, 19119–19129. [CrossRef] [PubMed]
30. Du, L.; Xie, Z.; Si, G.; Yang, A.; Li, C.; Lin, J.; Li, G.; Wang, H.; Yuan, X. On-Chip Photonic Spin Hall Lens. *ACS Photonics* **2019**, *6*, 1840–1847. [CrossRef]
31. Ohno, T.; Miyanishi, S. Study of surface plasmon chirality induced by Archimedes' spiral grooves. *Optics Express* **2006**, *14*, 6285–6290. [CrossRef] [PubMed]
32. Tan, Q.; Guo, Q.; Liu, H.; Huang, X.; Zhang, S. Controlling the plasmonic orbital angular momentum by combining the geometric and dynamic phases. *Nanoscale* **2017**, *9*, 4944–4949. [CrossRef]